

## Article

# Actual Marine Atmospheric Pre-Corrosion Fatigue Performance of 7075-T73 Aluminum Alloy

Laixin Shi <sup>1,\*</sup>, Lin Xiang <sup>2,\*</sup>, Jianquan Tao <sup>2</sup>, Qiang Chen <sup>2</sup>, Jun Liu <sup>2</sup> and Yong Zhong <sup>2</sup>

<sup>1</sup> College of Material Science and Engineering, Chongqing University of Technology, Chongqing 400054, China

<sup>2</sup> Southwest Technology and Engineering Research Institute, Chongqing 400039, China; jarryallen@163.com (J.T.); 2009chenqiang@hfut.edu.cn (Q.C.); bvvh\_liu@163.com (J.L.); wanshi3816@163.com (Y.Z.)

\* Correspondence: shilaixin2016@cqut.edu.cn (L.S.); xlin0731@163.com (L.X.); Tel.: +86-15123376156 (L.S.); +86-18792897339 (L.X.)

**Abstract:** Actual marine atmospheric pre-corrosion behavior and its effect on the fatigue performance of 7075-T73 aluminum alloy were studied by means of marine atmospheric outdoor exposure testing and fatigue testing. The surface and cross-sectional microstructures of aluminum alloy specimens after different numbers of days of exposure were analyzed. Localized pitting, and intergranular and exfoliation corrosion occurred during the outdoor exposure of aluminum alloy specimens in a marine atmosphere. The degree of severity of atmospheric corrosion increased with increasing duration of exposure. The effects of Fe-rich constituent particles ( $\text{Al}_{23}\text{CuFe}_4$ ) and grain boundary precipitates ( $\text{MgZn}_2$ ) on the marine atmospheric corrosion behavior were discussed. In addition, when the exposure time was increased from 0 days to 15 days, the average fatigue life of aluminum alloy specimens decreased dramatically from about  $125.16 \times 10^4$  cycles to  $16.58 \times 10^4$  cycles. As the exposure time was further increased to 180 days, the average fatigue life slowly decreased to about  $6.21 \times 10^4$  cycles. The fatigue fracture characteristics and the effect mechanism of marine atmospheric pre-corrosion on the fatigue life of 7075-T73 aluminum alloy were also analyzed.

**Keywords:** 7075 aluminum alloy; outdoor exposure; actual marine atmosphere; pre-corrosion; fatigue



**Citation:** Shi, L.; Xiang, L.; Tao, J.; Chen, Q.; Liu, J.; Zhong, Y. Actual Marine Atmospheric Pre-Corrosion Fatigue Performance of 7075-T73 Aluminum Alloy. *Metals* **2022**, *12*, 874. <https://doi.org/10.3390/met12050874>

Academic Editor: George A. Pantazopoulos

Received: 10 April 2022

Accepted: 19 May 2022

Published: 21 May 2022

**Publisher's Note:** MDPI stays neutral with regard to jurisdictional claims in published maps and institutional affiliations.



**Copyright:** © 2022 by the authors. Licensee MDPI, Basel, Switzerland. This article is an open access article distributed under the terms and conditions of the Creative Commons Attribution (CC BY) license (<https://creativecommons.org/licenses/by/4.0/>).

## 1. Introduction

The aluminum alloy 7075 has received a great deal of attention because of its outstanding properties, which include low density and high strength; therefore, it has been used widely as a structural material in the aircraft industry [1–6]. However, when aircraft are in service, especially in marine atmospheric environments, the aluminum alloy structures used inevitably suffer atmospheric corrosion damage, which could significantly degrade the fatigue performance and reduce the service life of those structures [7–9]. Thus, a better understanding of the effect of marine atmospheric corrosion on the fatigue performance of 7075 aluminum alloy would be vitally important and helpful in furthering research on the service safety and life cycle of aircraft structures.

To date, many studies have been performed elucidating the effects of pre-corrosion on the fatigue performance of 7075 aluminum alloy [10–22]. For instance, Sankaran et al. [12] investigated the effects of pitting pre-corrosion on the fatigue behavior of aluminum alloy 7075-T6 using cyclic fog–dry salt spray tests, and found that the fatigue lives of aluminum alloys could be dramatically reduced by pitting corrosion. Burns et al. [16] studied the effect of EXCO solution pre-corrosion on the fatigue cracking of 7075-T6511 aluminum alloy and reported that the substantial reduction in fatigue life due to pre-corrosion was nearly independent of pre-corrosion time after an initial sharp degradation. Joshi et al. [19] used constant stress amplitude fatigue tests to study the small crack growth behavior of pre-corroded aluminum alloy 7075-T6 and found that small crack initiation life and

crack growth life under salt water conditions were several times shorter than those under ambient air. However, the investigations of the impact of pre-corrosion on the fatigue performance of 7075 aluminum alloy performed so far have mainly employed accelerated corrosion methods to simulate atmospheric corrosion in the laboratory, seldom employing marine atmospheric exposure tests, which in practice are more reliable and accurate for evaluating actual marine atmospheric corrosion. Zhang et al. [23] performed atmospheric exposure tests of epoxy primer-coated 7075-T6 aluminum alloy in a coastal environment and found that the epoxy coating and anodic oxide layer had lost their protective ability after 20 years of exposure.

However, the investigations that have been performed so far have mainly focused on 7075-T6 (peak-aged) aluminum alloy, and have seldom addressed 7075-T73 (over-aged) aluminum alloy, which may have a lower strength and better corrosion resistance than 7075-T6 alloy [24]. In fact, to the best of our knowledge, the pre-corrosion fatigue performance of bare 7075-T73 aluminum alloy exposed outdoors in an actual marine atmosphere for short durations such as several days remains unclear. In this work, we investigate the marine atmospheric corrosion behavior of bare 7075-T73 aluminum alloy by means of outdoor exposure tests in an actual marine atmosphere at the Wanning test site. The fatigue performance of atmospheric pre-corrosion aluminum alloy specimens with different durations of outdoor exposure was also analyzed by means of constant amplitude axial fatigue tests. The corrosion characteristics and fatigue fracture of pre-corrosion aluminum alloy specimens were observed. In addition, the mechanisms of actual marine atmospheric corrosion and the effect of pre-corrosion on fatigue life are discussed.

## 2. Experimental Procedure

The aluminum alloy specimens used in this work were cut from an extruded 7075-T73 aluminum alloy sheet along the extrusion direction, and its chemical composition (wt.%) is indicated in Table 1. Figure 1 shows the geometry and dimensions of the specimens exposed to actual marine atmospheric environment. The average value of the yield strength and tensile strengths of the 7075-T73 aluminum alloy specimens were measured to be about 490 MPa and 562 MPa, respectively.

**Table 1.** Chemical composition (wt.%) of the 7075-T73 aluminum alloy.

| Element             | Zn   | Mg   | Cu   | Fe   | Ti    | Si    | Cr   | Mn    | Al   |
|---------------------|------|------|------|------|-------|-------|------|-------|------|
| Weight fraction (%) | 5.57 | 2.58 | 1.51 | 0.14 | 0.024 | <0.05 | 0.20 | 0.045 | Bal. |

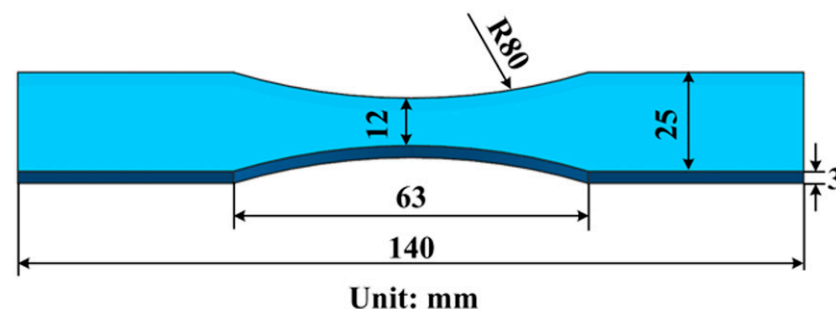


**Figure 1.** Geometry and dimensions of the 7075-T73 aluminum alloy specimens.

All tests of outdoor exposure in actual marine atmosphere were carried out at Wanning test site in China, which is close to the South China Sea. The average air temperature, relative humidity, and  $\text{Cl}^-$  deposition rate at the Wanning test site can reach about 23.9 °C, 87.6% and 14.5875 mg/(m<sup>2</sup> d), respectively [23], indicating that this marine atmosphere environment is characterized by high temperature, high humidity, and high salt fog. The aluminum alloy specimens were installed on the test rack, which was facing south at an angle of 45° and situated 350 m away from the coastline. The selected specimens were

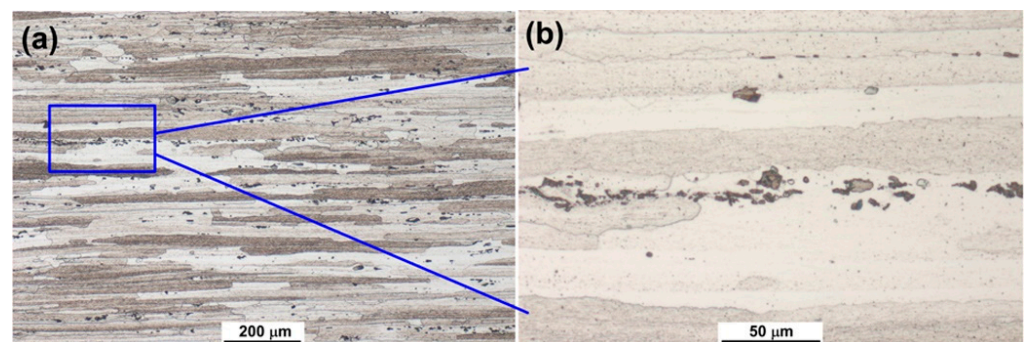
exposed to the actual marine atmosphere for 15, 30, 90 and 180 days, respectively. After the outdoor exposure tests, the obtained atmospherically pre-corroded specimens were withdrawn from the Wanning test site and kept in a desiccator (DZF-6020, Hefei Kejing Materials Technology Co., Ltd., Hefei, China). Afterwards, fatigue tests were carried out on the atmospherically pre-corroded specimens that had been exposed for various duration under constant amplitude axial loading on a QBG-50 fatigue testing machine (Changchun Qianbang, Changchun, China) in laboratory air at room temperature to determine their fatigue life. Sine wave load and a maximum cyclic stress ( $S_{\max}$ ) of 240 MPa were applied in all the fatigue tests. Moreover, the stress ratio (R) was set as 0.1 and the loading frequency was about 80 Hz. The fatigue tests were repeated at least five times for each type of marine atmospherically pre-corroded specimen.

In addition, selected as-received (uncorroded) and atmospherically pre-corroded aluminum alloy specimens were cross-sectioned, ground, polished and then etched for microstructural observation using an optical microscope (OM, DMI5000M, Leica, Wetzlar, Germany) and a scanning electron microscope (SEM, Evo18, Carl Zeiss, Germany) equipped with energy disperse spectroscopy (EDS). Selected samples were also cut from the as-received and pre-corroded specimens in order to analyze their surface morphologies and fatigue fracture characteristics using SEM (secondary electron and backscattered electron) and EDS. The thin foils were mechanically thinned to a thickness of 100  $\mu\text{m}$  before being twin-jet electro-polished in a solution consisting of 5% perchloric acid and 95% ethanol for microstructural analysis of the as-received specimens using a transmission electron microscope (TEM, JEM-2100, JEOL Ltd., Tokyo, Japan).

### 3. Results and Discussion

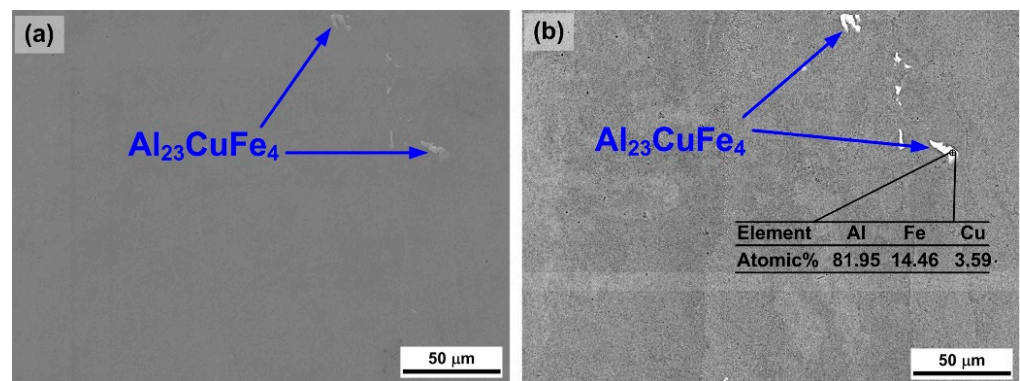
#### 3.1. Microstructures of As-Received 7075 Aluminum Alloy

Figure 2 displays the OM microstructure of as-received 7075 aluminum alloy. As indicated, the microstructure contains many elongated grains that are parallel to the extrusion direction of the aluminum alloy. In addition, several second-phase constituent particles can be observed within the grain or near the grain boundary.



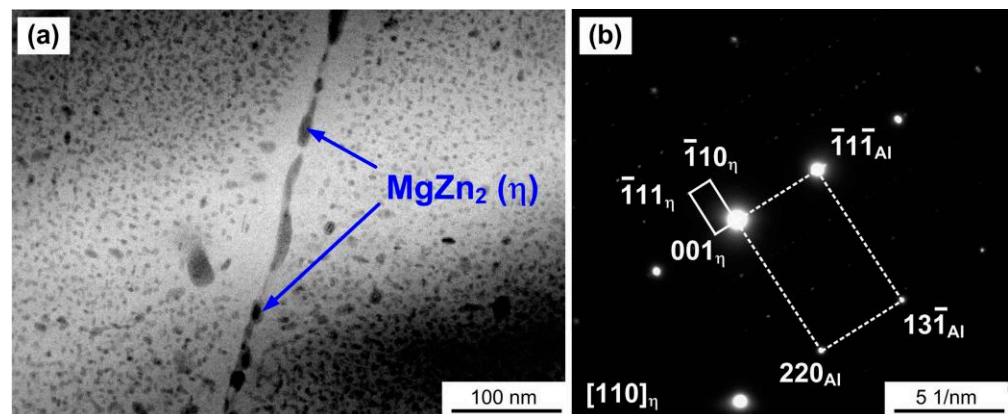
**Figure 2.** OM microstructures of as-received 7075 aluminum alloy. Image (b) shows the magnified microstructure in the frame area of image (a).

Figure 3 shows the surface morphology of the as-received 7075 aluminum alloy. It can be seen that the as-received alloy surface is free from corrosion and relatively smooth. Moreover, some second-phase constituent particles can also be observed on the alloy surface. According to previous studies [25–27], the constituent particles in 7075 aluminum alloy might be Fe-rich phase ( $\text{Al}_{23}\text{CuFe}_4$  or  $\text{Al}_7\text{Cu}_2\text{Fe}$ ). The EDS results in Figure 3b further indicate that the chemical composition of these constituent particles was  $\text{Al}_{23}\text{CuFe}_4$ .



**Figure 3.** Surface morphology of as-received 7075 aluminum alloy: (a) secondary electron image and (b) backscattered electron image.

Figure 4 shows the TEM microstructure of the 7075-T73 aluminum alloy. It is clear that a lot of fine second-phase precipitates are distributed homogeneously within the aluminum alloy matrix. In addition, a continuous chain of precipitates can also be observed at the grain boundaries. The electron diffraction pattern (Figure 4b) reveals that the grain boundary precipitates are  $\text{MgZn}_2$  ( $\eta$ ) phase.



**Figure 4.** TEM microstructure of the 7075-T73 aluminum alloy: (a) bright-field image and (b) electron diffraction pattern of grain boundary precipitates.

### 3.2. Corrosion Characteristics

Figure 5 shows the surface morphologies of 7075 aluminum alloy specimens exposed to marine atmosphere for different numbers of days. After 15 days of outdoor exposure, some pits with various sizes and irregular shape can be observed on the surface of the aluminum alloy specimen, suggesting that localized pitting corrosion has occurred. The atmospheric corrosion products in the pitting corrosion regions can be seen as having a black appearance in the SEM backscattered electron images (Figure 5b,d). The EDS results show that these atmospheric corrosion products mainly contain the elements O and Al. According to the ratio of Al to O, it can be deduced that the corrosion products of the 7075 aluminum alloy specimens suffering from marine atmospheric pre-corrosion mainly consist of  $\text{Al}(\text{OH})_3$  [23]. Furthermore, as shown in Figure 5c,d, some atmospheric corrosion products might be washed away by rainwater, and the mud-crack characteristic can be observed on the surface of the remaining corrosion products. After 30 days of outdoor exposure, the number and size of the pits increase, and the mud-crack characteristic of corrosion product surface becomes more obvious, as shown in Figure 5e–h. When the outdoor exposure time is increased to 90 days, the severity of the localized atmospheric corrosion on the surface of the aluminum alloy specimens increases. The adjacent pits tend to interact with each other, and the size of the pits further increases, as shown in Figure 5i–l.

After 180 days of outdoor exposure, most of the aluminum alloy specimen surface suffers from atmospheric corrosion. As indicated in Figure 5m–p, the size of the pits increases significantly, which can be attributed to adjacent pits converging into larger pits. Moreover, there are some newly formed small pits on the specimen surface. It is worth noting that, as shown in Figure 5, several corrosion pits are distributed close to the Fe-rich constituent particles ( $\text{Al}_{23}\text{CuFe}_4$ ). Accordingly, it can be inferred that the occurrence of localized pitting corrosion on the surface of 7075-T73 aluminum alloy specimens exposed to the marine atmosphere is closely associated with the Fe-rich constituent particles, which might have higher electrochemical potential than the surrounding aluminum alloy matrix [25].

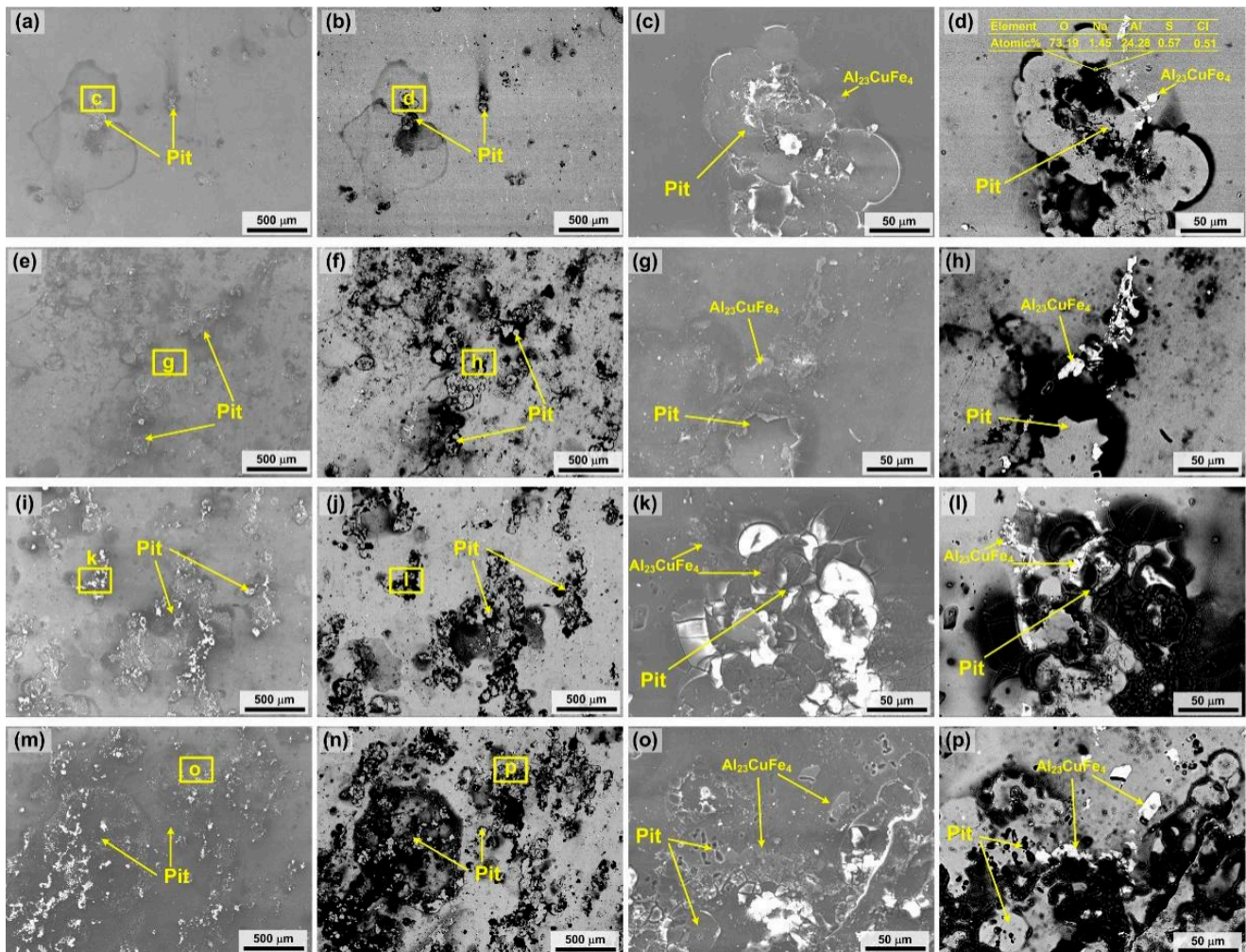


**Figure 5.** SEM secondary electron and backscattered electron images of the surface morphologies of 7075 aluminum alloy specimens exposed outdoor for different numbers of days: (a–d) 15 days; (e–h) 30 days; (i–l) 90 days; (m–p) 180 days.

Figure 6 shows the cross-sectional microstructures of 7075 aluminum alloy specimens subjected to outdoor exposure for different numbers of days. As indicated, there is no obvious corrosion in the as-received specimen (see Figure 6a). After 15 days of outdoor exposure, as shown in Figure 6b,f, localized intergranular corrosion can be seen to have occurred in the aluminum alloy matrix, and lamellar cracks extend along the elongated grain boundary parallel to the alloy surface. The EDS results presented in Figure 6f show that the intergranular corrosion products are also mainly  $\text{Al}(\text{OH})_3$ . After 30 days of outdoor exposure, both the length and depth of the intergranular corrosion have increased (see Figure 6c). With further increases in the duration of outdoor exposure, the degree of severity of the intergranular corrosion progressively increases. When the duration of

outdoor exposure is increased to 180 days, the corrosion layers near the surface of the aluminum alloy specimens come apart and are even exfoliated (see Figure 6e), indicating that exfoliation corrosion is occurring.

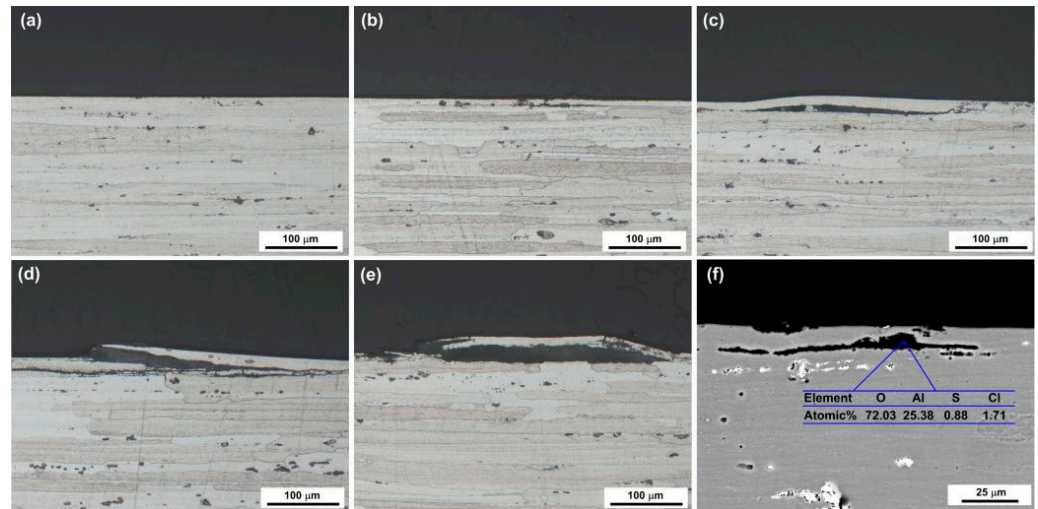


**Figure 6.** (a–e) OM and (f) backscattered electron images for the cross-sectional microstructures of 7075 aluminum alloy specimens subjected to outdoor exposure for different numbers of days: (a) 0 days; (b,f) 15 days; (c) 30 days; (d) 90 days; (e) 180 days.

As mentioned above, pitting, intergranular, and exfoliation corrosion may occur in the 7075-T73 aluminum alloy specimens exposed to the actual marine atmosphere at the Wanning test site, which has a high humidity and high chlorine ion ( $\text{Cl}^-$ ) concentration. Under the conditions of the marine atmospheric environment, the oxide film on the surface of the 7075 aluminum alloy specimen, especially close to the Fe-rich constituent particles, might be damaged by electrolyte water films containing  $\text{Cl}^-$ , and then the aluminum alloy matrix is exposed directly to marine atmosphere. Because the electrochemical potential of the Fe-rich constituent particles is different from that of the aluminum alloy matrix [25], electrochemical reactions between them may occur. Compared with the Fe-rich constituent particles, the surrounding aluminum alloy matrix with lower electrochemical potential acts as an anode, and would be dissolved preferentially, leading to the occurrence of pitting corrosion.

In addition, intergranular and exfoliation corrosion of the exposed 7075-T73 aluminum alloy specimens might be related to the precipitates at the grain boundaries. As mentioned above, in the 7075-T73 aluminum alloy, the precipitates at the grain boundaries were identified as  $\text{MgZn}_2$  phase (see Figure 4). Under the action of corrosive media in the actual marine atmosphere, an electrochemical corrosion system might be formed by the  $\text{MgZn}_2$  grain boundary precipitates and the aluminum alloy matrix. It has been reported that  $\text{MgZn}_2$  phase has a lower electrochemical potential than the aluminum alloy matrix [28]. Therefore, in the above electrochemical corrosion system, the  $\text{MgZn}_2$  precipitates at the grain boundaries act as the anode and are dissolved preferentially, resulting in the occurrence of intergranular corrosion. As the intergranular corrosion proceeds along the elongated grain boundaries parallel to the specimen surface, the corrosion products will accumulate at the grain boundaries. The volume of corrosion products ( $\text{Al}(\text{OH})_3$ ) will be larger than that of the consumed aluminum alloy matrix [29,30]. As a result, wedging force might be generated at the elongated grain boundaries, which could cause the rupture and exfoliation of the alloy surface. Accordingly, exfoliation corrosion occurs in the 7075-T73 aluminum alloy specimen subjected to outdoor exposure for 180 days, as shown in Figure 6e.

### 3.3. Fatigue Performance

Figure 7 shows the average fatigue lives of the 7075-T73 aluminum alloy specimens subjected to outdoor exposure in marine atmosphere for different numbers of days. The maximum cyclic stress ( $S_{\max}$ ) was 240 MPa. As indicated, the average fatigue life ( $N_f$ ) of the uncorroded aluminum alloy specimens was about  $125.16 \times 10^4$  cycles. After 15 days of outdoor exposure, the average  $N_f$  of the pre-corroded aluminum alloy specimens had significantly decreased to about  $16.58 \times 10^4$  cycles, indicating that low-level marine atmospheric corrosion damage was able to dramatically reduce the fatigue life of the 7075-T73 aluminum alloy specimens. After the initial sharp degradation, with increasing outdoor exposure duration, the average fatigue life of the aluminum alloy specimens still progressively decreased, but the rate of decrease became much smaller. Thus, the average  $N_f$  of pre-corroded aluminum alloy specimens decreased from about  $16.58 \times 10^4$  cycles to about  $6.21 \times 10^4$  cycles when number of days of exposure increased from 15 to 180.

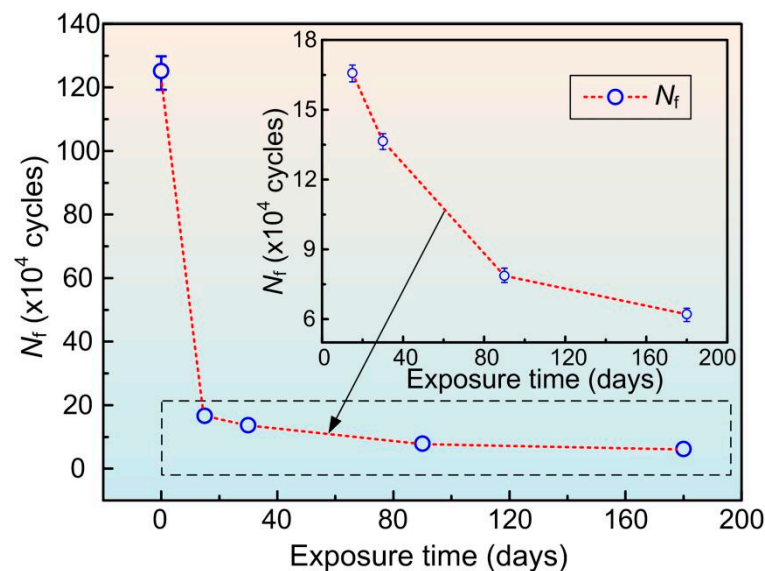


**Figure 7.** Average fatigue life ( $N_f$ ) of the 7075 aluminum alloy specimens subjected to outdoor exposure for different numbers of days.

Figure 8 shows the fatigue fracture morphologies of 7075 aluminum alloy specimens subjected to outdoor exposure for different numbers of days. It can be seen that, in the absence of pre-corrosion, the fatigue crack initiated at a Fe-rich constituent particle ( $\text{Al}_{23}\text{CuFe}_4$ ) near the surface of the aluminum alloy specimen, as shown in Figure 8a–c. The Fe-rich constituent particles are harder than the aluminum alloy matrix and can give rise to stress concentration. Thus, they could act as an initiation site for fatigue cracking. After 15 days of outdoor exposure, the fatigue crack originated from a shallow localized corrosion region near the corner of the pre-corroded aluminum alloy specimen, as shown in Figure 8d–f. When the outdoor exposure duration increased to 180 days, the initiation site of the fatigue crack revealed an irregular deep localized corrosion feature that was also situated near the corner of the alloy specimen, as shown in Figure 8g–i.

As can be seen from the experimental results, marine atmospheric corrosion can penetrate the surface of aluminum alloy specimens and change the initiation site of fatigue cracking. The stress concentration caused by the generation of localized atmospheric corrosion regions during outdoor exposure in the marine atmosphere could significantly accelerate the initiation of fatigue cracks. Therefore, the fatigue life of atmospherically pre-corroded 7075-T73 aluminum alloy specimens with 15 days of exposure was dramatically reduced compared with that of the uncorroded specimens (see Figure 7). With the prolongation of the duration of atmospheric pre-corrosion, the depth of the localized pre-corroded region increased progressively, as shown in Figure 8d–i, which might further

increase the severity of stress concentration and thus reduce the initiation time of fatigue cracking. However, the contribution of the increase in the depth of localized pre-corrosion region to the decrease in the fatigue life might be weaker than that of the generation of the localized pre-corrosion region. As a consequence, the fatigue life of the atmospherically pre-corroded 7075-T73 aluminum alloy specimens decreased slowly when the duration of outdoor exposure was increased from 15 days to 180 days.

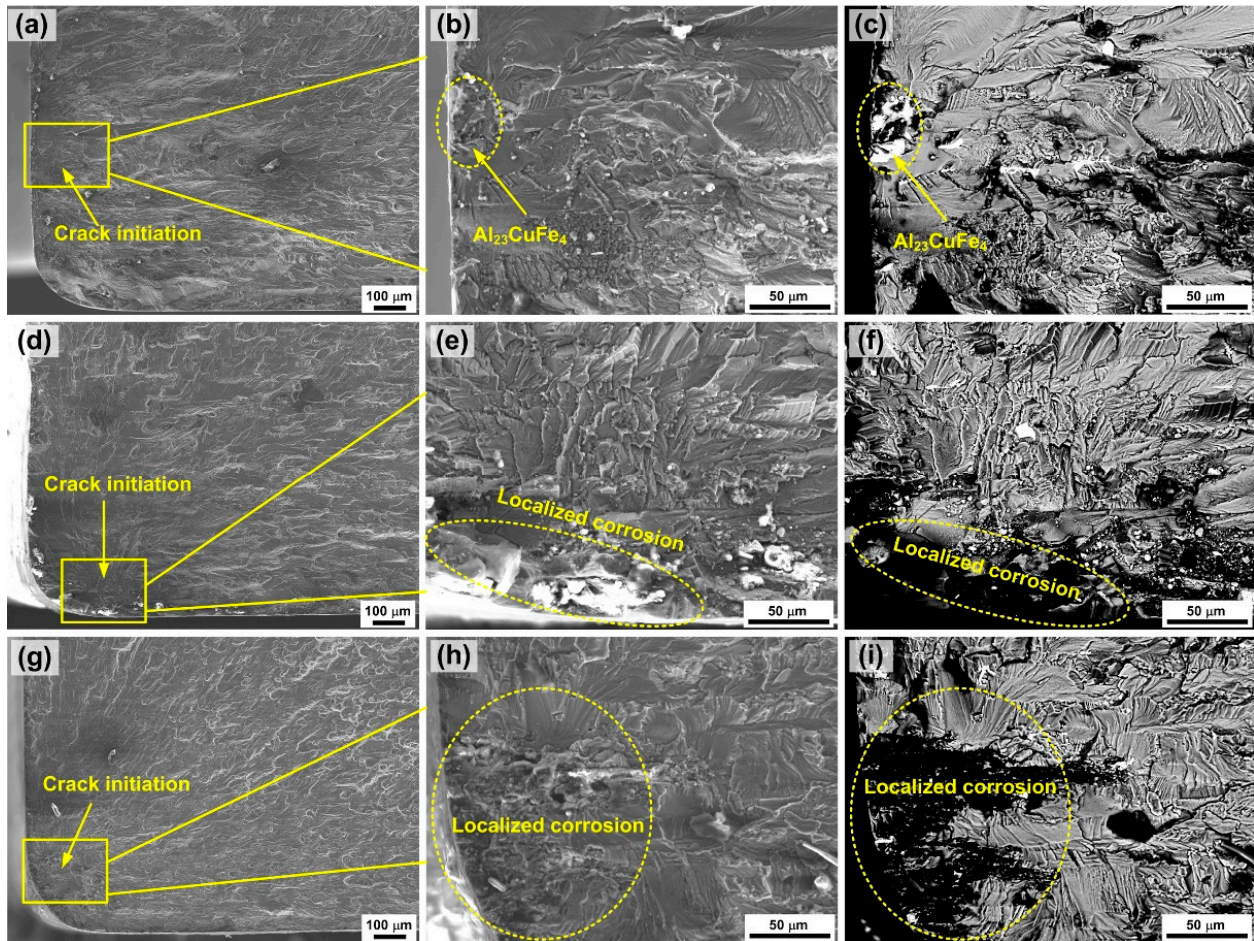


**Figure 8.** SEM secondary electron and backscattered electron images of fatigue fracture morphologies of 7075-T73 aluminum alloy specimens exposed outdoor for different days: (a–c) 0 days; (d–f) 15 days; (g–i) 180 days.

#### 4. Conclusions

(1) When the 7075-T73 aluminum alloy specimen was subject to outdoor exposure in actual marine atmosphere for a short duration (no more than 15 days), localized pitting and intergranular corrosion occurred near the alloy surface. The degree of severity of marine atmospheric corrosion increased with increasing exposure duration. After 180 days of outdoor exposure, exfoliation corrosion also took place.

(2) The formation of corrosion pits was mainly attributed to the anodic dissolution of the matrix around the Fe-rich constituent particles ( $\text{Al}_{23}\text{CuFe}_4$ ). The intergranular corrosion and exfoliation corrosion were mainly related to the preferential anodic dissolution of  $\text{MgZn}_2$  ( $\eta$ ) phase precipitates at the elongated grain boundaries of the aluminum alloy.

(3) The fatigue cracking of the as-received (uncorroded) specimens was mainly initiated near the  $\text{Al}_{23}\text{CuFe}_4$  particles, causing stress concentration. With increasing exposure time, the fatigue life ( $N_f$ ) of the alloy specimens first decreased dramatically and then continued to decrease more slowly. The initial sharp decrease in  $N_f$  can be attributed to the generation of a localized pre-corrosion region, inducing more serious stress concentration

and thus significantly accelerating the initiation of fatigue cracking. The following slow decrease of  $N_f$  might be related to the increasing depth of the localized pre-corrosion region with the prolongation of exposure time.

**Author Contributions:** L.S. and L.X. conceived, designed, and performed the experiments; L.S., L.X., J.T. and Q.C. analyzed the data; J.L. and Y.Z. contributed reagents/materials/analysis tools; L.S. wrote the paper. All authors have read and agreed to the published version of the manuscript.

**Funding:** The work was supported by the Southwest Institute of Technology and Engineering Cooperation Fund (Grant No. HDHDW5902020105) and the Basic and Advanced Research Project of CQ CSTC (Grant No. cstc2018jcyjAX0035).

**Institutional Review Board Statement:** Not applicable.

**Informed Consent Statement:** Not applicable.

**Data Availability Statement:** The data presented in this study are available on request from the corresponding author. The data are not publicly available due to privacy.

**Conflicts of Interest:** The authors declare no conflict of interest.

## References

1. Georgantzia, E.; Gkantou, M.; Kamaris, G.S. Aluminium alloys as structural material: A review of research. *Eng. Struct.* **2021**, *227*, 111372. [[CrossRef](#)]
2. Zhou, B.; Liu, B.; Zhang, S.G. The advancement of 7xxx series aluminum alloys for aircraft structures: A review. *Metals* **2021**, *11*, 718. [[CrossRef](#)]
3. Dursun, T.; Soutis, C. Recent developments in advanced aircraft aluminium alloys. *Mater. Des.* **2014**, *56*, 862–871. [[CrossRef](#)]
4. Li, Y.; Retraint, D.; Gao, P.; Xue, H.; Gao, T.; Sun, Z. Effect of surface mechanical attrition treatment on torsional fatigue properties of a 7075 aluminum alloy. *Metals* **2022**, *12*, 785. [[CrossRef](#)]
5. Jung, D.K.; Ha, S.H.; Kim, H.K.; Shin, Y.C. Determination of plastic anisotropy of extruded 7075 aluminum alloy thick plate for simulation of post-extrusion forming. *Metals* **2021**, *11*, 641. [[CrossRef](#)]
6. Chen, F.; Qu, H.; Wu, W.; Zheng, J.H.; Qu, S.; Han, Y.; Zheng, K. A physical-based plane stress constitutive model for high strength AA7075 under hot forming conditions. *Metals* **2021**, *11*, 314. [[CrossRef](#)]
7. Su, J.X.; Zou, Y.; Chen, K.M.; Wang, Z.Y.; Guan, Q.F. Corrosion mechanism and characteristic of 7075-T6 aluminum alloy panel on airline aircraft. *J. Mech. Eng.* **2013**, *49*, 91–96. [[CrossRef](#)]
8. Zhang, R.X.; Zhao, W.D.; Zhang, H.; Yang, W.J.; Wang, G.X.; Dong, Y.L.; Ye, C. Fatigue performance rejuvenation of corroded 7075-T651 aluminum alloy through ultrasonic nanocrystal surface modification. *Int. J. Fatigue* **2021**, *153*, 106463. [[CrossRef](#)]
9. Barter, S.A.; Molent, L. Service fatigue cracking in an aircraft bulkhead exposed to a corrosive environment. *Eng. Fail. Anal.* **2013**, *34*, 181–188. [[CrossRef](#)]
10. Huang, Y.; Ye, X.; Hu, B.; Chen, L. Equivalent crack size model for pre-corrosion fatigue life prediction of aluminum alloy 7075-T6. *Int. J. Fatigue* **2016**, *88*, 217–226. [[CrossRef](#)]
11. Obert, B.; Ngo, K.; Hashemi, J.; Ekwaro-Osire, S.; Sivam, T.P. An investigation of the reduction in tensile strength and fatigue life of pre-corroded 7075-T6 aluminum alloy. *J. Mater. Eng. Perform.* **2000**, *9*, 441–448. [[CrossRef](#)]
12. Sankaran, K.K.; Perez, R.; Jata, K.V. Effects of pitting corrosion on the fatigue behavior of aluminum alloy 7075-T6: Modeling and experimental studies. *Mater. Sci. Eng. A* **2001**, *297*, 223–229. [[CrossRef](#)]
13. DuQuesnay, D.L.; Underhill, P.R.; Britt, H.J. Fatigue crack growth from corrosion damage in 7075-T6511 aluminium alloy under aircraft loading. *Int. J. Fatigue* **2003**, *25*, 371–377. [[CrossRef](#)]
14. Jones, K.; Hoepfner, D.W. Pit-to-crack transition in pre-corroded 7075-T6 aluminum alloy under cyclic loading. *Corros. Sci.* **2005**, *47*, 2185–2198. [[CrossRef](#)]
15. Genel, K. The effect of pitting on the bending fatigue performance of high-strength aluminum alloy. *Scr. Mater.* **2007**, *57*, 297–300. [[CrossRef](#)]
16. Burns, J.T.; Kim, S.; Gangloff, R.P. Effect of corrosion severity on fatigue evolution in Al-Zn-Mg-Cu. *Corros. Sci.* **2010**, *52*, 498–508. [[CrossRef](#)]
17. Burns, J.T.; Larsen, J.M.; Gangloff, R.P. Driving forces for localized corrosion-to-fatigue crack transition in Al-Zn-Mg-Cu. *Fatigue Fract. Eng. Mater. Struct.* **2011**, *34*, 745–773. [[CrossRef](#)]
18. Zupanc, U.; Grum, J. Effect of pitting corrosion on fatigue performance of shot-peened aluminium alloy 7075-T651. *J. Mater. Process. Technol.* **2010**, *210*, 1197–1202. [[CrossRef](#)]
19. Joshi, G.; Mall, S. Crack Initiation and growth from pre-corroded pits in aluminum 7075-T6 under laboratory air and salt water environments. *J. Mater. Eng. Perform.* **2017**, *26*, 2293–2304. [[CrossRef](#)]
20. McMurtrey, M.D.; Bae, D.; Burns, J.T. Fracture mechanics modelling of constant and variable amplitude fatigue behaviour of field corroded 7075-T6511 aluminium. *Fatigue Fract. Eng. Mater. Struct.* **2017**, *40*, 1–18. [[CrossRef](#)]

21. Song, H.P.; Liu, C.C.; Zhang, H.; Du, J.; Yang, X.D.; Leen, S.B. In-situ SEM study of fatigue micro-crack initiation and propagation behavior in pre-corroded AA7075-T7651. *Int. J. Fatigue* **2020**, *137*, 105655. [[CrossRef](#)]
22. Song, H.P.; Liu, C.C.; Zhang, H.; Yang, X.D.; Chen, Y.J.; Leen, S.B. Experimental investigation on damage evolution in pre-corroded aluminum alloy 7075-T7651 under fatigue loading. *Mater. Sci. Eng. A* **2021**, *799*, 140206. [[CrossRef](#)]
23. Zhang, S.; Zhang, T.; He, Y.T.; Du, X.; Ma, B.L.; Zhang, T.Y. Long-term atmospheric pre-corrosion fatigue properties of epoxy primer-coated 7075-T6 aluminum alloy structures. *Int. J. Fatigue* **2019**, *129*, 105225. [[CrossRef](#)]
24. Rometsch, P.A.; Zhang, Y.; Knight, S. Heat treatment of 7xxx series aluminium alloys—Some recent developments. *Trans. Nonferr. Met. Soc. China* **2014**, *24*, 2003–2017. [[CrossRef](#)]
25. Pao, P.S.; Feng, C.R.; Gil, S.J. Corrosion fatigue crack initiation in aluminum alloys 7075 and 7050. *Corrosion* **2000**, *56*, 1022–1031. [[CrossRef](#)]
26. Pao, P.S.; Gill, S.J.; Feng, C.R. On fatigue crack initiation from corrosion pits in 7075-T7351 aluminum alloy. *Scr. Mater.* **2000**, *43*, 391–396. [[CrossRef](#)]
27. Birbilis, N.; Cavanaugh, M.K.; Buchheit, R.G. Electrochemical behavior and localized corrosion associated with Al<sub>7</sub>Cu<sub>2</sub>Fe particles in aluminum alloy 7075-T651. *Corros. Sci.* **2006**, *48*, 4202–4215. [[CrossRef](#)]
28. Wang, Z. *Handbook of Aluminum Alloy and Its Working*; Central South University Press: Changsha, China, 2000.
29. Mcnaughtan, D.; Worsfold, M.; Robinson, M.J. Corrosion product force measurements in the study of exfoliation and stress corrosion cracking in high strength aluminium alloys. *Corros. Sci.* **2003**, *45*, 2377–2389. [[CrossRef](#)]
30. Robinson, M.J.; Jackson, N.C. The influence of grain structure and intergranular corrosion rate on exfoliation and stress corrosion cracking of high strength Al-Cu-Mg alloys. *Corros. Sci.* **1999**, *41*, 1013–1028. [[CrossRef](#)]